

**QC
807.5
.U66
no.456**

NOAA Technical Report OAR 456-SEC 42



RADIATION DAMAGE OF THE PROTON MEPED DETECTOR ON POES (TIROS/NOAA) SATELLITES

M. Galand
D. Evans

February 2000

U.S. DEPARTMENT OF COMMERCE
National Oceanic and Atmospheric Administration
Space Environment Center

NOAA Technical Report OAR 456-SEC 42



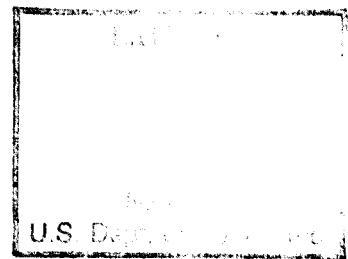
RADIATION DAMAGE OF THE PROTON MEPED DETECTOR ON POES (TIROS/NOAA) SATELLITES

Marina Galand
David Evans

Space Environment Center
Boulder, Colorado

February 2000

QC
807.5
.466
no. 456



U.S. DEPARTMENT OF COMMERCE
William M. Daley, Secretary

National Oceanic and Atmospheric Administration
D. James Baker, Under Secretary for Oceans and Atmosphere/Administrator

Oceanic and Atmospheric Research Laboratories
Silver Spring, Maryland
David L. Evans, Director

**National Oceanic and Atmospheric Administration
TIROS Satellites and Satellite Meteorology**

ERRATA NOTICE

One or more conditions of the original document may affect the quality of the image, such as:

Discolored pages

Faded or light ink

Binding intrudes into the text

This has been a co-operative project between the NOAA Central Library and the Climate Database Modernization Program, National Climate Data Center (NCDC). To view the original document contact the NOAA Central Library in Silver Spring, MD at (301) 713-2607 x124 or Library.Reference@noaa.gov.

HOV Services
Imaging Contractor
12200 Kiln Court
Beltsville, MD 20704-1387
January 26, 2009

NOTICE

Mention of a commercial company or product does not constitute an endorsement by the NOAA Oceanic and Atmospheric Research Laboratories. Use of information from this publication concerning proprietary products or the test of such products for publicity or advertising purposes is not authorized.

For sale by the National Technical Information Service, 5285 Port Royal Road
Springfield, VA 22061

TABLE OF CONTENTS

<i>Abstract.</i>	<i>1</i>
<i>1. Introduction</i>	<i>2</i>
<i>2. MEPED instrument description</i>	<i>3</i>
2.1 POES satellite	3
2.2 Proton MEPED detector	4
2.3 Data collection	5
<i>3. Investigation of damage</i>	<i>5</i>
3.1 Is the detector degraded over time?	5
3.2 Rate of degradation	6
<i>4. Origin of the damage</i>	<i>9</i>
4.1 Dead layer and partial charge collection	9
4.2 Particles causing the damage	10
<i>5. Conclusions and discussion</i>	<i>11</i>
<i>Acknowledgments.</i>	<i>12</i>
<i>Appendix 1. Programs developed</i>	<i>13</i>
A1.1 Fortran programs for reading the MEPED data from the 16s-data files (also called CDF files) and analyzing them	13
A1.2 Idl routines for the visualization	14
<i>References</i>	<i>16</i>
<i>Figures from 1 to 8</i>	<i>17</i>

Abstract.

The Medium Energy Proton and Electron Detector (MEPED), aboard the polar-orbiting, low-altitude, POES (Polar Operational Environmental Satellite) and measuring protons in the 30 keV-6 MeV energy range, undergoes damage over time. During all phases of solar activity, its response in auroral latitudes decreases as much as 90% over time. This decrease is caused by radiation damage. The 90° detector observes larger fluxes of protons which mirror at or below the satellite than the 0° detector which observes smaller fluxes of auroral precipitating protons in the loss cone. For this reason the 90° detector suffers from radiation damage much faster than the 0° detector. In addition, the damage effects can be seen earlier, when the satellite is launched near solar maximum, and damage effects during major magnetic storms can be observed in the data. The high radiation dose the MEPED instrument undergoes over the years causes the formation of a dead layer in the silicon structure and a partial charge collection. As a result, the energy of the incident proton, as well as the particle flux, is underestimated in auroral regions. This shift in energy is dependent on the proton energy. In addition, even though the protons measured by the MEPED instrument contribute to the damage, they are not the only ones. Further investigation must be undertaken concerning the particles responsible for the damage in order to correlate the shift in energy with the total counts of particles. In the meantime, one can bypass the damage effect by rejecting data obtained in the late life of the satellite, the period of rejection varying from one satellite to another.

1. Introduction

The Medium Energy Proton and Electron Detector (MEPED) instrument is aboard the National Oceanic and Atmospheric Administration (NOAA) Polar Operational Environmental Satellites (POES). These satellites were previously known as Television and InfraRed Observation Satellites (TIROS). The MEPED measures the intensities of charged particle radiation from 30 keV to greater than 200 MeV. These high-energy particles can greatly affect the environment, and may be of serious concern in space weather. For example, when such particles reach a satellite, there is a possibility of disruption of its system with surface and deep dielectric charging induced by energetic electrons, and penetration of the instruments by the high energy protons. In addition, when precipitating down to the ionosphere, energetic electrons and protons produce ionization in the mesosphere and low thermosphere [Codrescu *et al.*, 1997], which causes disturbances of radio communications like the long distance VLF signals propagating in the Earth-Ionosphere wave guide. Moreover, the MeV proton radiation represents a hazard for astronauts, especially in the area of the South Atlantic anomaly. Therefore it is useful to monitor and study these particles to determine the cause of anomalies in satellites and degradation of radio communications, and in support of NASA's manned space missions.

In a study using the NOAA 6 satellite, *Lyons and Evans* [1984] presented data from the proton MEPED instrument. In one of the plots of their Figure 2 valid in the auroral region, the intensity of protons measured in the loss cone is much larger than the intensity of protons which mirror below the satellite. While magnetic-field aligned distributions are expected for electrons owing to effective electric fields, it is difficult to believe this would be the case for ions, except rarely, because their pitch angle distribution is induced by wave scattering. The unexpected relative intensities observed could be due to damage of the detector over the years, and the search for an explanation has motivated the present study.

After a brief description of the space-borne MEPED instrument and the data collection, we investigate the possibility of damage undergone by the proton MEPED detector and we study the rate of degradation between the 0° and the 90° instruments. Next we discuss the origin of the damage. Finally, we propose possible future steps to this study. Note that the information about the different software programs developed for use in the present study can be found in Appendix 1.

2. MEPED instrument description

2.1 POES satellite

The **POES** satellites, also known as **TIROS/NOAA**, have a sun-synchronous, circular, polar, low-altitude orbit with a 98° inclination. The satellites thus move from the east towards the west and always cross the equator northbound at the same local time. Their orbital period is about 105 min and their approximate altitude is 850 km (topside *F*-layer) [Raben *et al.*, 1995].

The POES satellites carry a set of instruments called the Space Environment Monitor (**SEM**) to detect and monitor the influx of ions and electrons into the upper atmosphere as a result of solar and magnetospheric activity [Raben *et al.*, 1995]:

- the Total Energy Detector (**TED**) is an electrostatic analyzer observing protons or electrons in 11 energy bands between 300 eV and 20 keV, for two viewing angles, at 0° , that is radially outward along the Earth-satellite vector, and at 30° ,
- the Medium Energy Proton and Electron Detector (**MEPED**) is a solid-state detector measuring protons between 30 keV and a few MeV in five bands or electrons above 30 keV in three bands, for two viewing angles, 0° and 90° with respect to the zenith. In addition, there are three omnidirectional dome solid-state detectors that measure the intensity of protons from 16 to greater than 215 MeV.
- the High Energy Proton and Alpha Detector (**HEPAD**) senses the intensity in the local zenith direction of ambient solar protons above 370 MeV in four bands and of ambient alpha particles above 640 MeV per nucleon in two energy bands. The HEPAD was only operating aboard TIROS N and NOAA 6.

As we are investigating possible radiation damage of the MEPED detector, the satellites selected for the present study have a relatively long history of data for this instrument: TIROS N - here called NOAA 0 -, NOAA 6, NOAA 10, and NOAA 12. The period of MEPED data collected over the years is presented in [Table 1](#). Note that the end date for NOAA 12 is not the last operating date as the SEM system is still in operation and will be on future POES missions.

The **age** of the satellite is defined with respect to the start of collection of useable MEPED data (second column in Table 1). There is some overlap between NOAA 0 and NOAA 6 and between NOAA 6 and NOAA 10, which allows us to compare detectors of different ages.

Table 1. Satellites selected in the present study (first column) with the period of data obtained for the MEPED proton detector (second and third columns). The total number of years of data used here is given for each satellite in the last column.

NOAA satellite Name	Start date of MEPED data	End date of MEPED data	Number of years of MEPED data
NOAA 0 (TIROS N)	November 2, 1978	February 27, 1981	2.3
NOAA 6	July 8, 1979	November 16, 1986	7.4
NOAA 10	October 12, 1986	May 7, 1991	4.6
NOAA 12	June 3, 1991	December 14, 1998	7.4

2.2 Proton MEPED detector

The MEPED detector is a solid-state detector measuring either electrons or ions/neutrals. There is no mass discrimination; the ions (which could be He⁺ or O⁺) are here assumed to be only protons. Moreover, there is no discrimination between neutral atoms and ions. But, at the altitude of the satellite, the atmosphere is not very dense, so that the proportion of precipitating neutrals (H atoms) is expected to be very low, because charge-exchange processes are not efficient here. There are two detectors for each charge type (electrons or protons) aboard the satellite. The **0° detector** views radially outward along the Earth-satellite vector, while the **90° detector** views in a perpendicular direction to the first one and to the satellite velocity vector. The field of view being $\pm 14^\circ$, the 0° detector views downward going particles with pitch angles less than 20° (in the northern hemisphere) at high latitudes. Therefore, in this region, the 0° detector is observing charged particles in the loss cone (precipitating particles), whereas the 90° detector views particles which mirror at or below the satellite [above the dense atmosphere] (trapped particles).

In the present study we focus on the **proton MEPED 0° and 90° detectors**. They measure protons in five energy bands: **30-80 keV, 80-250 keV, 250-800 keV, 800 keV-2.5 MeV, 2.5-6 MeV**. These instruments are solid-state silicon detectors, as illustrated in [Figure 1](#). A proton impacts the silicon atoms, liberating free electrons. One electron-hole pair is released per 3.2 eV of incident energy. It is a linear detector, that is, it produces a quantity of charge directly proportional to the quantity of energy deposited in the active volume of the detector by the incident particle. In addition, an electric field is applied such that the free electrons are directed to a capacitor that feeds an amplifier. The voltage pulse is proportional to the amount of charge collected during

10 ns, which helps insure the measurement of energy from a single incident proton. Finally, electronic analysis of the pulse identifies the proton within one of the five energy bands. A 2500-gauss magnetic field is imposed across the aperture structure of the proton detector to prevent electrons of energy lower than 1.5 MeV from reaching the silicon detector. Moreover, the front face of the detector is coated with an aluminum layer, which serves both as an electrical contact and a suppressor of the detector's sensitivity to photons. However, unlike the electron MEPED instrument, the proton detector has no nickel foil covering it to block light and low energy protons.

2.3 Data collection

The particle counts are recorded every 2 s with an integration time of 1 s, for the five proton energy bands and for both directions of observation. An **average over 16 s** is applied to these data, which corresponds to approximately 100 km of satellite track, or about 1° latitude at mid-latitude locations. The response of the detector for a given energy band and viewing direction is then provided in counts/s and stored on CD-ROMs [Raben *et al.*, 1995]. These data are used in the present study. Applying a geometrical factor equal to $9.5 \times 10^{-3} \text{ cm}^2 \text{ sr}$ (that is a multiplication factor of 105), the response for a given energy band can be converted into protons $\text{cm}^{-2} \text{ s}^{-1} \text{ sr}^{-1}$.

3. Investigation of damage

3.1 Is the detector degraded over time?

Figure 2 shows the 90° proton detector response, averaged over a day in the auroral regions, as a function of the age of the satellite (as defined in section 2.1), for the four selected satellites. The auroral region is defined as that for which $4 < L < 15$, where L is approximately equal to the distance in Earth's radii of the equatorial crossing of the associated magnetic field line. The energy band selected for display in Figure 2 is 30-80 keV, because it records the highest count rate in auroral regions, so it is a good monitor of the medium energy proton flux.

The times of minimum and maximum of the solar cycles are given in Table 2 and shown on the plots of Figure 2.

Table 2. Solar sunspot cycle number and years of the associated minimum and maximum.

Solar sunspot cycle number	Year of minimum sunspot number	Year of maximum sunspot number
21	1976.5	1979.9
22	1986.8	1989.6
23	1996.7	

The **90° proton detector response dramatically decreases over time** for the four satellites. This decrease reaches values as much as 90%. It should be mentioned here that the **0° proton detector response** has the same trend but decreases slower. Moreover, NOAA 6 was launched during solar maximum, so the decrease of the proton detector response might be thought to be related to the decrease of solar activity. But this decrease is also observed for NOAA 10, which was launched at solar minimum. Therefore the decrease of the proton detector responses does not seem to be solely associated with the solar cycle. The **origin of the decrease** observed on the four satellites is rather **related to degradation of the MEPED instrument over the years**.

3.2 Rate of degradation

Figure 3 shows the total cumulative counts of the 0° and 90° proton detectors, associated with the four first energy bands. Over time, the 90° detector accumulates many more counts than the 0° detector. Because the most probable damage is from radiation, we would expect that the 90° detector would deteriorate faster than the 0° detector.

In order to investigate this point further, we define an **event** using the three following criteria:

(1) Minimum value for the proton detector response (read in the 16s-data file):

- 0° detector response > 100 counts/s
- 90° detector response > 100 counts/s

(2) Observations in the auroral regions

- $L > 4$, that is $|\text{Geomagnetic latitude}| > \sim 60^\circ$
- Polar cap excluded, that is exclude $L > 15$

(3) \square Greater value for the 0° proton detector response compared with that of the 90° detector:

$$\triangleright \quad \text{Ratio} = \frac{0^\circ \text{response}}{90^\circ \text{response}} > 1.2$$

Figure 4 shows the **percentage, per day, of occurrence of the third criterion (3)**, when the first two (1) and (2) are satisfied. This percentage of occurrence, noted α , is defined as the ratio (multiplied by 100) of the number, per day, of events (that is, the number, per day, of cases for which the three criteria are satisfied) to the number, per day, of cases for which only the first two criteria are satisfied. As mentioned in the introduction, the pitch angle distribution of the auroral protons is induced by wave scattering. Therefore we expect an event to occur only rarely. This is what is observed at the early age of NOAA 10, for example, for which the percentage α is close to 0%. But, at the same time, for NOAA 6, whose MEPED instruments have already been in operation for 2500 days, the percentage α is close to 100%. The comparison between NOAA 6 and NOAA 10 shows that this high value obtained at the end of the life of NOAA 6 cannot be explained by the environmental effects alone. A similar comparison can be performed for NOAA 0 and 6, and for NOAA 10 and 12. We have here another **confirmation that the MEPED detector undergoes deterioration due to aging**. The general trend observed for the four satellites in Figure 4 is an increase of the percentage α with the age of the satellite. This demonstrates the **relatively accelerated degradation of the 90° detector compared with the 0° detector**. Note that this increase is closely related to the solar cycle. Indeed, the increase is much faster for NOAA 6 and NOAA 12, launched near solar maximum, compared with that obtained for NOAA 10 launched during solar minimum. Moreover, for NOAA 10, the percentage α dramatically increases just after a huge magnetic storm, that of March 13, 1989 ($A_p=246$).

Beside this general trend, two particularities can be observed. First, we notice that the percentage α of NOAA 0 is of the order of 50% from the beginning. The satellite was launched on October 13, 1978, less than one month before the first useable data of the MEPED instrument, and no large solar flares or geomagnetic disturbances were reported for this period. On the other hand, the proton MEPED instruments aboard NOAA 0 are the only ones which were calibrated before launch. A calibration appropriate to the use of an ion beam was performed at Goddard Space Flight Center (NASA/GSFC). Perhaps the instruments received an excessive dose of radiation during this operation. However, to date, the question remains open. The second particularity which can be observed in Figure 4 is the decrease of the percentage α at an advanced age of NOAA 12. By looking at the history of the threshold calibrations of NOAA 12, we notice that in the past 3 years or so, the threshold for the 0° proton

detector has crept up, yielding an underestimation of the incident proton energy, while the 90° proton detector threshold has stayed about the same. As we explain in section 4.1, an increase in the effective energy threshold leads to a decrease of the counts in auroral latitudes. Therefore the deviation of the 0° proton detector threshold can explain this “recovery”, that is, the decrease of the percentage α . Nevertheless, the origin of the threshold enhancement remains unknown. On the other hand, the increase observed after the sharp decrease of the percentage α can be related to a strong magnetic storm occurring on August 26, 1998 for which the Ap index was of the order of 140. Finally, we would like to mention that the **periods when no data** were acquired for the MEPED instrument (**darkest boxes** in Figure 4) are still periods during which the detector might have undergone radiation damage, because there is no protection at the entrance to prevent particles from penetrating.

The ratio of the 0° to the 90° proton detector responses, during an event, as previously defined, and averaged over a day, is plotted in [Figure 5](#). For all four satellites, the ratio is increasing over time, **confirming that the 90° proton detector degrades faster than the 0° proton detector**. Note that the decrease for NOAA 12 can be related to that observed in Figure 4 and explained above. On the other hand, the rate of increase varies from one satellite to another. For example, the ratio for NOAA 6 reaches very high values after 1300 days of operation, while the increase for NOAA 10 is much smaller over the same lifetime. These different behaviors can be related to solar activity, as NOAA 6 was launched at solar maximum and NOAA 10 at solar minimum. A similar example is obtained with NOAA 10 and 12, the ratio for NOAA 12 increasing much more over time than that of NOAA 10. Following the launch of NOAA 12 in June 3, 1991, large solar flares were recorded and the months of June, July and October 1991 experienced strong magnetic activity with an index Ap sometimes between 120 and 200. In addition, the sharp increases in the NOAA 6 ratio are correlated with strong space environment disturbances. Between 1100 and 1200 days, the ratio enhancement occurs in the very active period of July-September 1982, with a culmination on September 6, 1982 (Ap=200) which results in an abrupt increase of the ratio. Around 2450 days, the ratio enhancement is correlated with the large magnetic storm of February 8, 1986 (Ap=200). On the other hand, during the operation time of NOAA 10, the severe magnetic storm of March 13, 1989 (Ap=246) had no effect on the ratio (even though its effect is visible in the percentage α of occurrence of the third criterion). We can conclude that **not only the present status of the space environment, but also the solar and magnetic history undergone by the satellite, are influencing the degradation rate**.

The analysis of the occurrence of the third criterion and of the 0° to 90° detector response ratio (Figures 4 and 5) allows us to confirm that the 90° detector is degraded

faster than the 0° detector. Because the 90° detector undergoes more radiation than the 0° one (Figure 3) and that the degradation is clearly related to the solar cycle and to magnetic activity (Figures 4 and 5), we can conclude that **the MEPED detectors undergo radiation damage over time.**

4. Origin of the damage

If we have demonstrated that the deterioration of the MEPED response is related to radiation damage, we need to propose an explanation concerning how the detector is damaged and to investigate further the type of particles causing this damage.

4.1 Dead layer and partial charge collection

Long-term, surface radiation on a solid-state detector, like the proton MEPED detector, yields:

- the formation of a so-called **dead layer**. By going through this damaged layer, the incident particle is slowed down, part of its energy being absorbed in the lattice of the damaged silicon, as illustrated in [Figure 6](#).
- a decrease of the mobility of the free electrons liberated in the crystal after impact by the incident proton. The free electrons take more time to reach the capacitor, leading to a **partial charge collection**.

As a result, fewer free electrons are collected within the 10 ns-integration time and then a smaller voltage pulse is generated, yielding an increase of the effective energy threshold, that is, an **underestimation of the energy of the incident proton**. The radiation damage effect is less for higher energy protons, simply because they penetrate deeper into the detector, where the radiation damage to the crystal structure is less. Therefore the shift in energy is dependent on the proton energy. Moreover, in the energy range of the MEPED instrument, **in the auroral region** the proton flux – or detector response - decreases with increasing energies. As a consequence, the underestimation of the proton energy means an **underestimation of the particle flux**, as illustrated in [Figure 7](#). Therefore the radiation damage leads to a decrease of the detector response over time in the auroral region, this result corroborating our first observations (cf. Figure 2).

4.2 Particles causing the damage

The higher the mass, the more effectively particles scatter off the massive silicon nuclei and then alter the crystalline structure. As a consequence, protons are more efficient than electrons at inducing radiation damage. Moreover, the electrons cannot be the cause of the radiation damage of the proton detector, because the strong magnetic field imposed across the aperture prevents most electrons from reaching the silicon. Another reason supporting this point is provided by the MEPED electron detector aboard the NOAA satellites. This detector does not seem to suffer badly from radiation damage; and, unlike the proton detector, it has nickel foil covering the silicon detector, which prevents any protons of energy below 135 keV reaching the crystal and which reduces considerably the energy flux of protons of higher energies.

Protons of energies between 50 keV up to 5 MeV can generate significant radiation damage in silicon surface-barrier detectors [Coleman *et al.*, 1968]. The MEPED instrument measures protons in precisely this energy range. Laboratory measurements show that the value of the time-integrated proton flux above which serious radiation damage effects can be seen (called total fluence) are about 10^{10} protons cm^{-2} (Hanser, personal communication, 1999). From Figure 3, at half lifetime, the total count is 50×10^{10} counts. Because the MEPED proton detector has a effective area of 25 mm^2 , the total flux of protons between 30 keV and 2.5 MeV is:

$$\frac{50 \times 10^{10}}{25 \times 10^{-2}} = 2 \times 10^{12} \text{ protons.cm}^{-2}, \text{ which is much higher than the minimum value noted}$$

above at which damage effects are seen. Therefore the proton flux measured by the MEPED detector is large enough to induce a serious damage of the instrument. If one assumes that only particles cause the damage, then the total number of particles counted by the MEPED instrument should be correlated with the increase of the damage, that is, with the percentage α of occurrence of the third criterion (see section 3.2). One could then estimate the radiation damage effect on the instrument by monitoring the total counts accumulated.

Figure 8 shows the percentage α of occurrence of the third criterion versus the total counts accumulated since the MEPED was put into service. There are some periods when no data were acquired but during which the detector was subjected to radiation (see darkest boxes in Figures 2, 4, and 5). Even though this lack of data affects the results shown in Figure 8 by underestimating the total counts after such a period of no recorded data, it does not change the conclusions. Moreover, the first four energy bands are taken into account, covering 30 keV up to 2.5 MeV, but whatever energy band is selected, the same trends are obtained. The slope and shape of the results vary from one satellite to another. For NOAA 6, launched during solar maximum, the

percentage α reaches high values for a much smaller total of counts compared to NOAA 10 launched during solar minimum. This means that, if the particles responsible for the damage are the protons measured by the MEPED instrument, the damage may not be a linear function of the total counts, but is a function of the count rate. Another explanation, a most probable one, is that the protons measured by the MEPED detector are not the only particles responsible for the radiation damage. Protons of lower energies could also participate in the deterioration of the instrument.

5. Conclusions and discussion

We have been able to demonstrate that the space-borne MEPED instrument detecting protons undergoes serious damage over time. Its response in auroral latitudes decreases as much as 90% over several years independent of the phase of the solar cycle (section 3.1). This damage is induced by a high radiation dose. The 90° detector, which undergoes more radiation, degrades faster than the 0° detector. In addition, the damage effects can be seen earlier when the instrument begins its journey in space close to a solar maximum. Finally, huge magnetic storms dramatically enhance the deterioration, even more when the instrument has already experienced a serious radiation dose at an earlier age (section 3.2).

The high radiation dose sustained by the MEPED instrument, a solid-state silicon detector, yields an increase of the effective energy threshold, that is, an underestimation of the energy of incident protons (section 4.1). In the auroral region where the proton flux is typically decreasing with increasing energy in the energy range of the MEPED (that is above 30 keV), this leads to an underestimation of the proton flux. As illustrated in Figure 2, the decrease of the proton flux over the years in auroral latitudes is significant, reaching values up to 90%. Since the 90° detector degrades faster than the 0° detector and the radiation damage induces an underestimation of the detector response in the auroral regions, over time the 0° detector response can become larger than the 90° detector response. The radiation damage can then explain the usual ratio, observed in the auroral regions by *Lyons and Evans* [1984], between the intensity of protons measured in the loss cone and the intensity of protons which mirror below the satellite.

In section 4.2, we have tried to identify the particles responsible for the damage. Protons in the MEPED energy range contribute to the instrument damage, but we have indicated that they are not the only ones. Protons of lower energy are likely also responsible for the damage. The electron MEPED detector, protected from low and medium energy protons, does not show any sign of serious aging damage.

At this stage of the study, laboratory experiments would be useful to identify more precisely the population responsible for the instrument damage. If such a population is monitored aboard the spacecraft, one might consider establishing a correlation between the radiation dose and the damage rate, especially between the radiation dose and the shift in energy observed over time. As explained in section 4.1, this shift is expected to be dependent on the proton energy. In the meantime, we can deal with the problem in the following way. From Figures 2, 4, and 5, we can estimate when the radiation damage starts to have a significant effect on the proton detectors, and then select a date after which the data are rejected. The 0° proton detector data can be used for a longer period, because it degrades slower compared to the 90° detector. Moreover, the period of useable data depends on the solar cycle. The useable period is longer for satellites launched during solar minimum, like NOAA 10, compared with that observed for satellites launched during solar maximum, like NOAA 6.

Acknowledgments.

M.G. would like to thank Sue Greer for her constant and valued support all along this study. M.G. also thanks Mihail Codrescu, Ted Fritz, Fred Hanser, and Herb Sauer for insightful discussions, as well as Rodney Viereck for providing magnetic activity information. M.G. gratefully acknowledges the financial support of the National Research Council and the Space Environment Center.

Appendix 1. Programs developed

A1.1 Fortran programs for reading the MEPED data from the 16s-data files (also called CDF files) and analyzing them

1) test_cdf.f

For a given NOAA satellite, the f77 program `test_cdf.f` reads the CDF files where the 16-s averaged MEPED data are stored and looks for the data related to auroral latitudes or to an *event* defined by (1), (2) and (3), before storing the information in different output files. The energy bands are selected inside the program. Note that this program needs the files `Makefile`, `cdfvars.h` and `dave_cdflib3` to be compiled. The compilation, linking and execution can be performed using `test_cdf_com`.

Input files:

- *INPUT*: are given the name of the selected satellite (Nxx) and the minimum ratio R of the 0° to the 90° detectors used to define an *event*, ratio typically taken equal to 1.2.
- *catalog_cdf*: are given the names of all the CDF files for all the satellites, files stored on CD Roms which are gathered in a tower.

Output files:

- *test_infoxx_out*: the 'xx' is the number of the selected satellite given in *INPUT*. This output file is a test to check the CDF files where MEPED data have been read.
- *test_noaaxx_out*: the 'xx' is the number of the selected satellite given in *INPUT*. In this output file, are stored the year, day, time, magnetic local time, L-value, the 90° and 0° proton detector responses, the 0° to 90° proton detector ratio, the 90°, and 0° electron detector responses, when the three criteria (1), (2), and (3) defining an *event* are satisfied.
- *test_noaaxx_out_bis*: the 'xx' is the number of the selected satellite given in *INPUT*. In this output file, are stored, as a function of day and year, the number of data obtained (for a given satellite, whatever the 0° to 90° proton detector ratio), the responses averaged over a day of the 0° and the 90° proton detectors, and the total count number or accumulated counts (since the starting date given in column 2 of Table 1) of the 0° and the 90° proton detectors. All of these quantities are valid for auroral region.

2) check.f

The f77 program **check.f** simply reads output files of the program **test_cdf** and counts the number of times every day the three criteria (1), (2), and (3) are satisfied. The compilation, linking and execution can be done using **check_com**.

Input files:

- *INPUT*: are given the name of the selected satellite (Nxx) and the minimum ratio R of the 0° to the 90° detectors used to define an *event*, ratio typically taken equal to 1.2.
- *test_noaaxx_out*, output of the program **test_cdf**. The 'xx' is the number of the selected satellite given in *INPUT*.

Output files:

- *check_noaaxx_out*: the 'xx' is the number of the selected satellite given in *INPUT*. For every year where data have been obtained for the selected satellite, are given the daily number of events, the responses averaged over a day of the 90° and the 0° proton detectors, their ratio, the 0° to 90° proton detector response ratio averaged over a day and the responses averaged over a day of the 90° and the 0° electron detectors, when the three criteria (1), (2), and (3) are satisfied.

A1.2 Idl routines for the visualization

During the execution of the following routines, one must enter the option for the output, 's' for screen and 'p' for postscript file.

1) read_data

The idl routine **read_data** allows to plot, for a given satellite and as a function of the age of the satellite, the percentage α , per day, of occurrence of the third criterion (when the two first ones are satisfied), the response of the 0° or 90° proton detector, and the 0° to 90° proton detector response ratio, these two last quantities averaged over a day with the three criteria satisfied. Are also plotted as a function of the age of the satellite, the response of the 0° or 90° proton detector averaged over a day in the auroral region.

Input files:

- *test_noaaxx_out_bis*, output file of the program **test_cdf.f**.
- *check_noaaxx_out*, output file of the program **check.f**.

2) survey

The *idl* routine **survey** is similar to **read_data** except it can be applied to several satellites at the same time. Three plates can be obtained: one showing the 90° proton detector response in auroral region, the other showing the 0° to 90° proton detector response ratio (when the three criteria are satisfied), and the third showing the percentage α of occurrence of the third criterion when the two first are satisfied. All these quantities are averaged over a day and plotted as a function of the age of the satellite.

Input files:

- *test_noaaxx_out_bis*, output file of the program **test_cdf.f**.
- *check_noaaxx_out*, output file of the program **check.f**.

3) survey_cor

The *idl* routine **survey_cor** allows to plot, for chosen satellites, two plates. The first one presents the 0° and 90° total counts accumulated since the MEPED instruments were in service, as a function of the age of the satellite. The second plate shows plots of the percentage α of occurrence of the third criterion when the two first are satisfied (averaged over a day), versus the total counts accumulated, for the 90° proton detector.

References

- Codrescu, M. V., T. J. Fuller-Rowell, R. G. Roble, and D. S. Evans, Medium energy particle precipitation influences on the mesosphere and lower thermosphere, *J. Geophys. Res.*, 102, 19,977-19,987, 1997.
- Coleman, J. A., D. P. Love, J. H. Trainor, and D. J. Williams, Effects of damage by 0.8 MeV-5.0 MeV protons in silicon surface-barrier detectors, *IEEE Trans. Nucl. Sci.*, NS-15, 363-372, 1968.
- Lyons, L. R., and D. S. Evans, An association between discrete aurora and energetic particle boundaries, *J. Geophys. Res.*, 102, 2395-2400, 1984.
- Raben, V. J., D. E. Evans, H. H. Sauer, S. R. Sahm, and M. Huynh, TIROS/NOAA satellite space environment monitor data archive documentation: 1995 update, *NOAA Tech. Memo.*, ERL SEL-86, 1995.

Figures from 1 to 8:

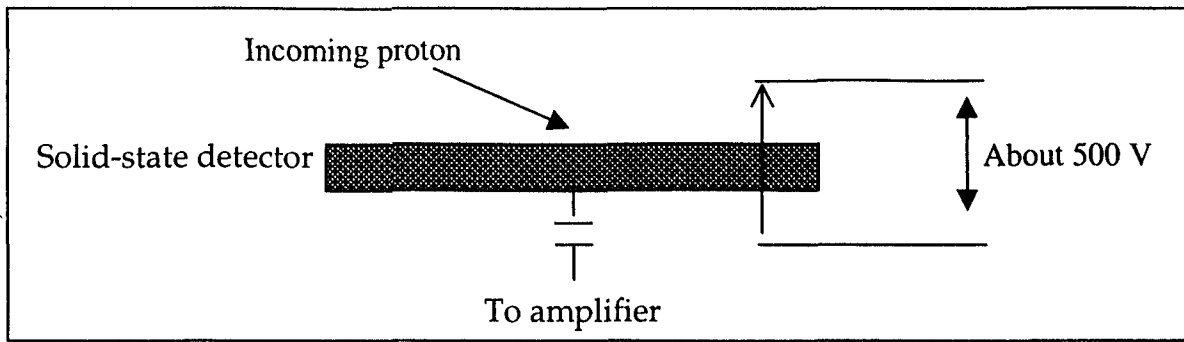


Figure 1. The proton MEPED detector is composed of a silicon solid-state detector of about 1 cm diameter and 0.05 mm thick. A high voltage is applied to the detector, generating an electric field which induces free electrons, liberated by impact of a proton on the silicon atoms, to enter a capacitor that feeds an amplifier.

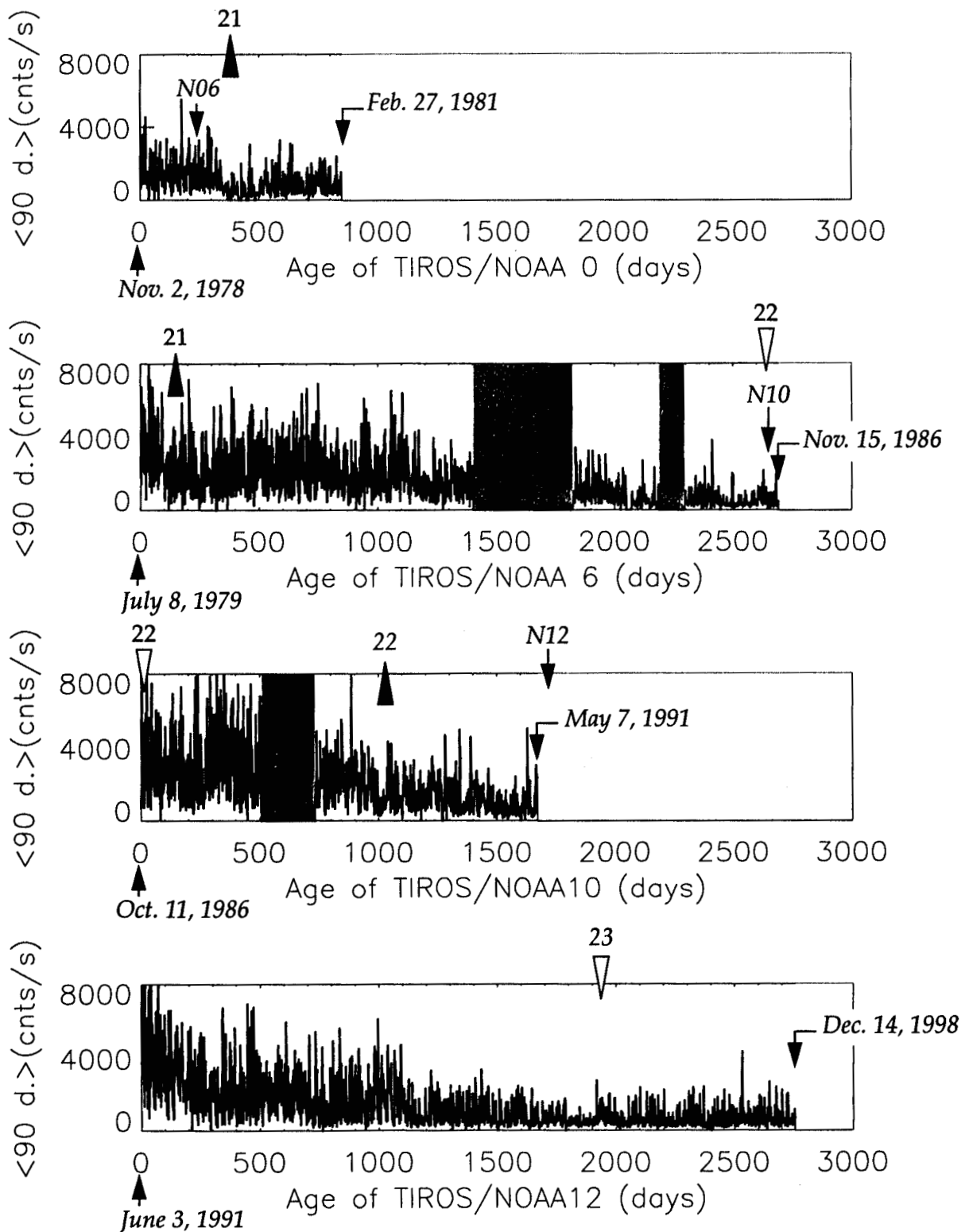


Fig.2: 90 degree proton detector response, averaged over a day in the auroral region, for the 30-80 keV energy band. The response is plotted, for NOAA 0, 6, 10, and 12, as a function of the age of the satellite, defined as the operation period of the MEPED instrument. The starting and stopping dates of operation are explicitly mentioned in *italic*. On the first three plots, the starting date of the next satellites, that is NOAA 6, 10 and 12, is shown with the name of the satellite in *italic*. The darkest boxes correspond to times where no data were acquired from the MEPED. The maximum and minimum of the solar cycles 21, 22, and 23 are shown with full upper triangles and empty down trian-

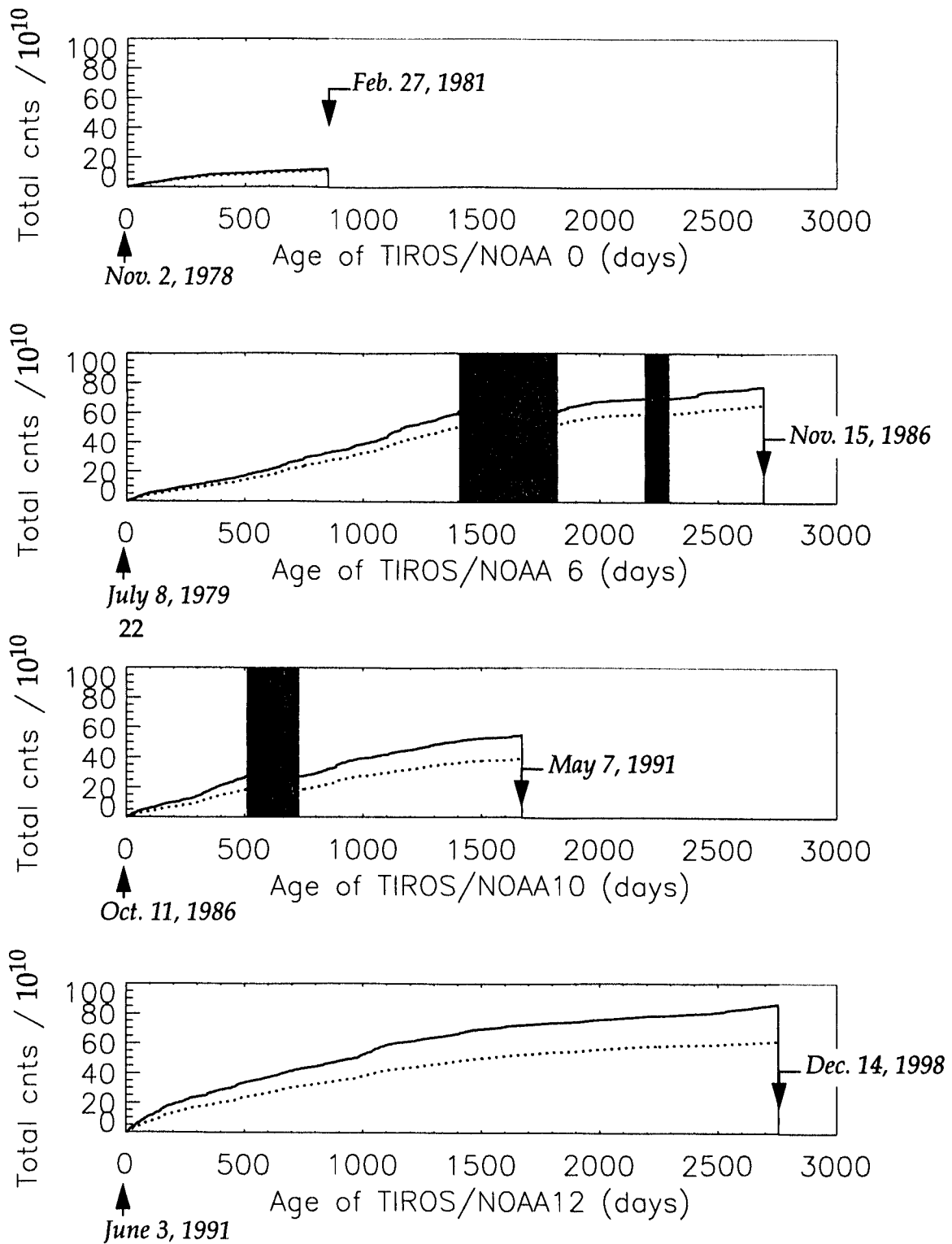


Fig.3: Total counts of the MEPED instrument accumulated over time, for NOAA 0, 6, 10 and 12 satellites. The data are from the four first energy bands covering the energy range from 30 keV to 2500 keV. The 0 and 90 degree detector responses are plotted with dotted and solid lines, respectively. The accumulated response is plotted as a function of the age of the satellite, defined as the operation period of the MEPED instrument. The starting and stopping dates are explicitly mentioned in italic. The darkest boxes correspond to times where no data were acquired from the MEPED.

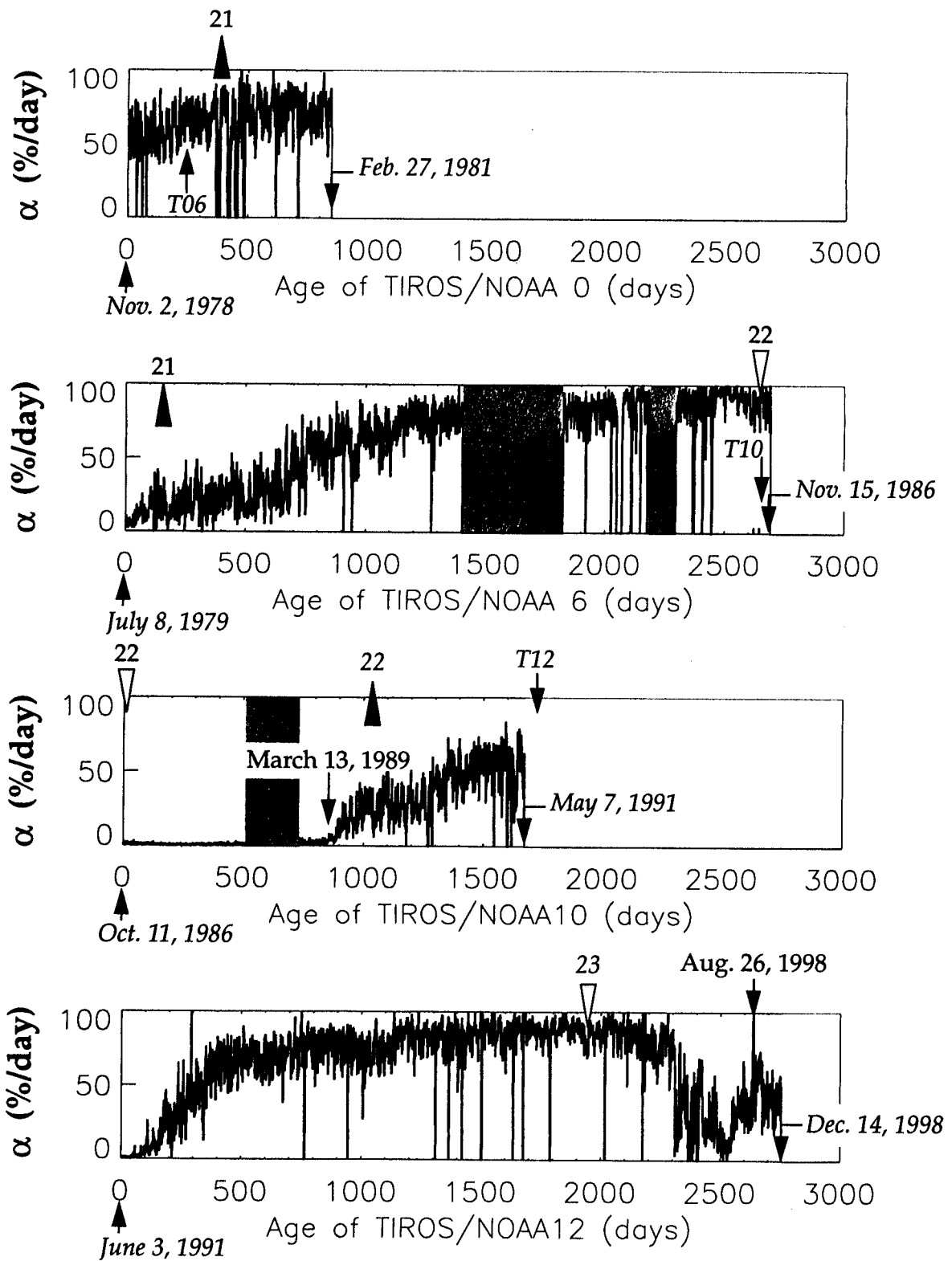


Fig.4: Percentage α of the occurrence of the third criterion, when the first two are satisfied. The data are from the 30-80 keV energy band of the MEPED instrument. The occurrence of event is plotted, for NOAA 0, 6, 10, and 12, as a function of the age of the satellite, defined as the operation period of the MEPED instrument. The starting and stopping dates are explicitly mentioned in *italic*. On the first three plots, the starting date of the next satellites, that is NOAA 6, 10 and 12, is shown with the name of the satellite in *italic*. The darkest boxes correspond to times where no data were acquired from the MEPED. The maximum and minimum of the solar cycles 21, 22, and 23 are shown with full upper triangles and empty down

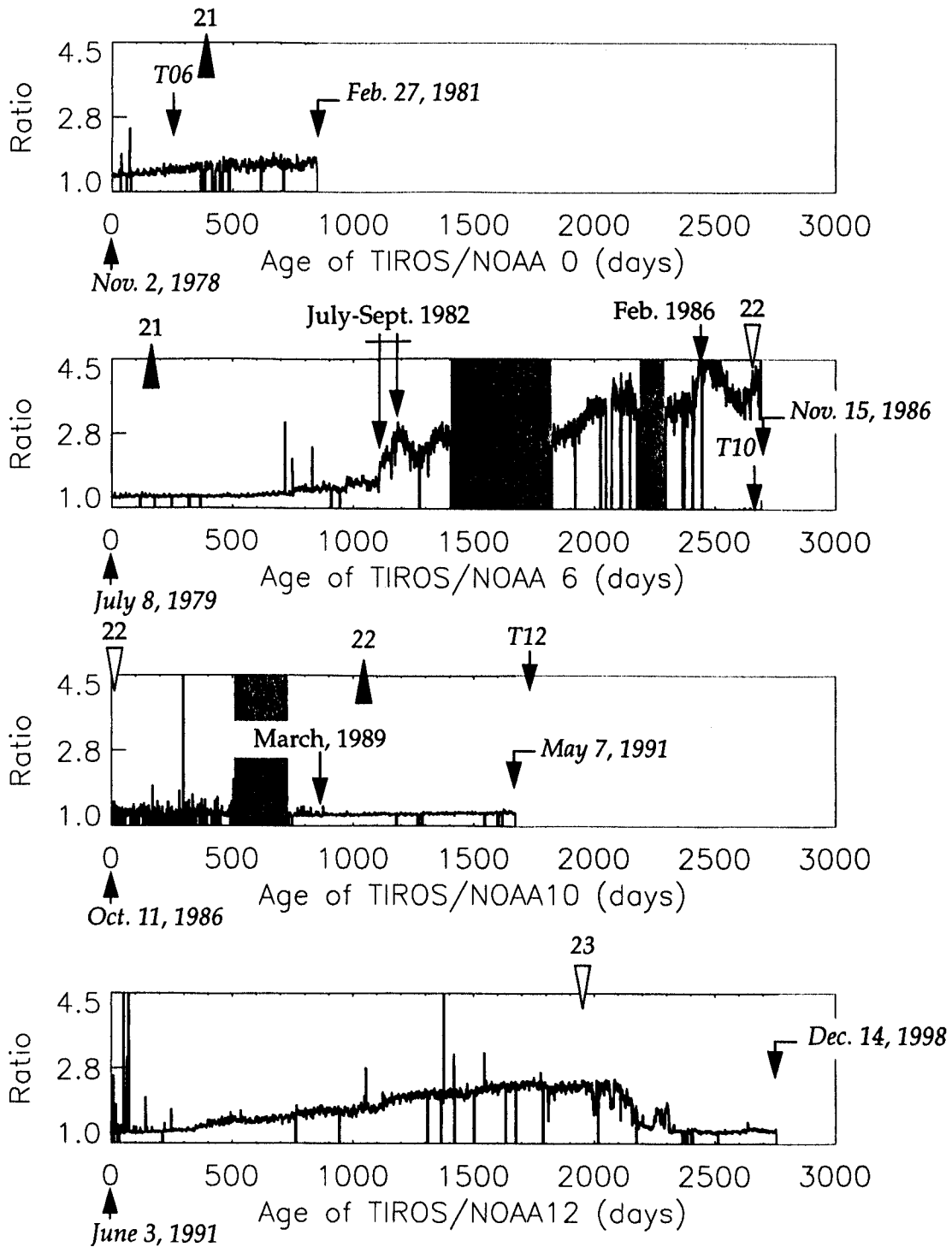


Fig.5: 0 degree detector response to 90 degree detector response ratio, during an event, and averaged over a day. The data are from the 30-80 keV energy band of the MEPED instrument. The ratio is plotted, for NOAA 0, 6, 10, and 12, as a function of the age of the satellite, defined as the operation period of the MEPED instrument. The starting and stopping dates are explicitly mentioned in *italic*. On the first three plots, the starting date of the next satellites, that is NOAA 6, 10 and 12, is shown with the name of the satellite in *italic*. The darkest boxes correspond to times where no data were acquired from the MEPED. The maximum and minimum of the solar cycles 21, 22, and 23 are shown with

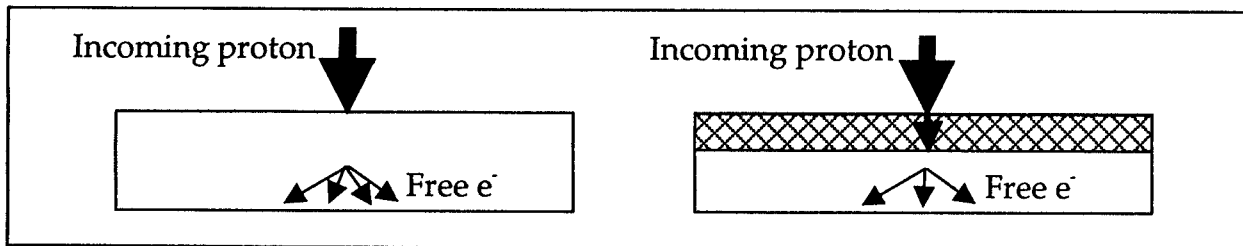


Figure 6. Incident energetic proton impacting a solid-state silicon detector before damage (left) and after the formation of a dead layer shown as the hatched rectangle (right). The result of the damage is a reduction of the number of free electrons liberated.

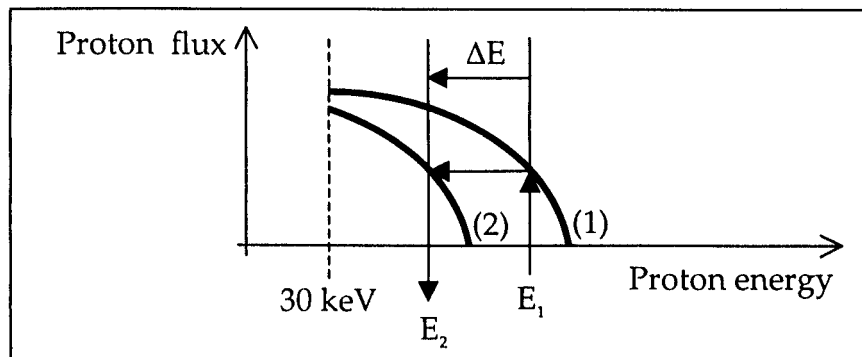


Figure 7. Proton flux as a function of the proton energy, in auroral regions, before (thick solid line (1)) and after (thick solid line (2)) the deterioration of the detector. After degradation, the instrument provides, for a given incident proton of energy E_1 , an energy E_2 with $E_2 < E_1$. The proton flux is shifted towards lower energies. As a result, because it is decreasing with increasing energies, the proton flux is underestimated.

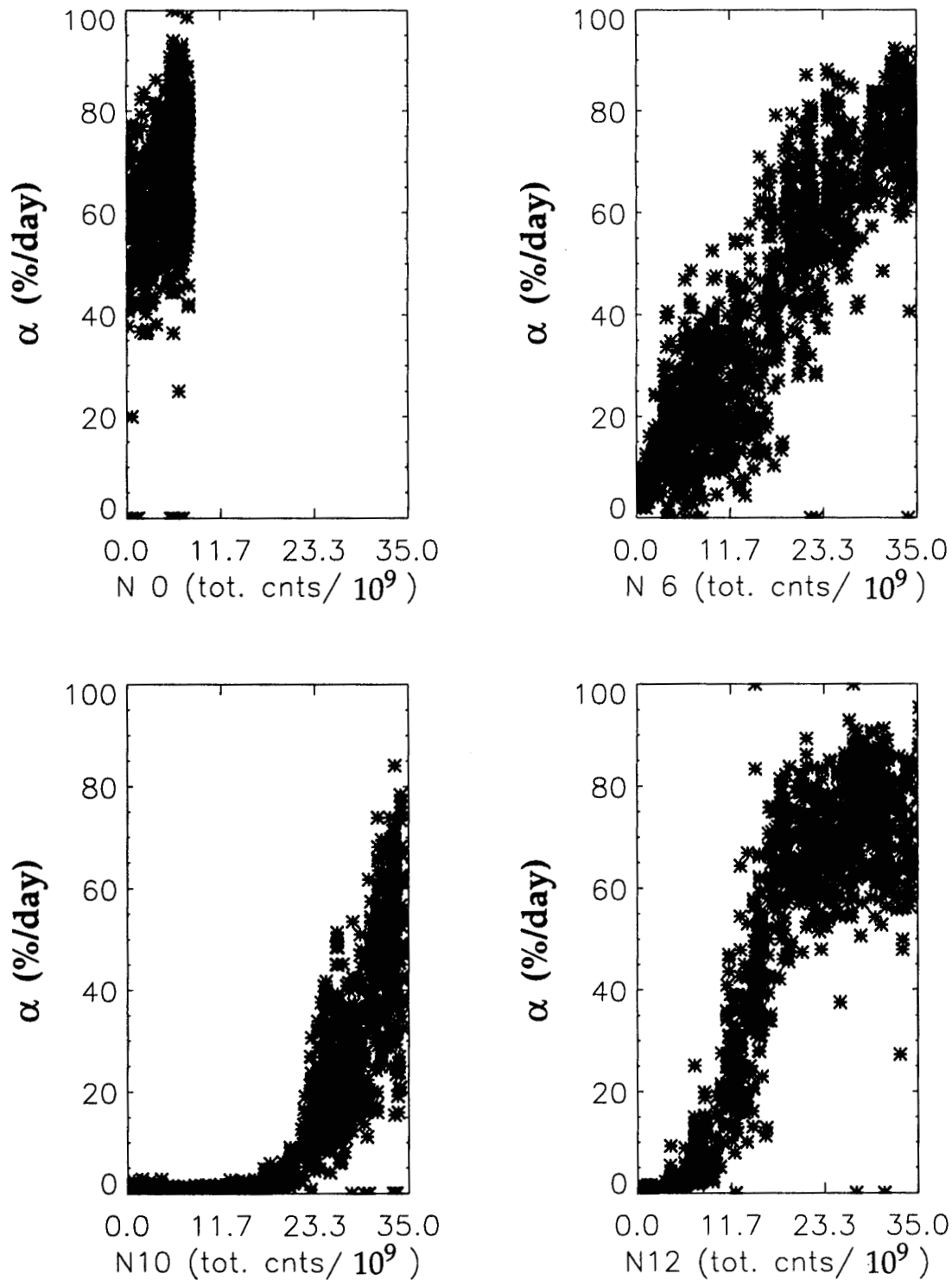


Figure 8: Percentage α of occurrence of the third criterion (when the two first ones are satisfied) versus the total counts accumulated since the MEPED instrument was put in service (second column of Table 1), for NOAA 0, 6, 10, and 12. The data are from the four first energy bands, covering the energy range from 30 keV to 2500 keV, of the 90 degree proton detector. 851 points (maximum reached) plotted for NOAA 0, 2000 points plotted for NOAA 6, 1674 points (maximum reached) plotted for NOAA 10, and 2000 points plotted for NOAA 12.